



TITLE:

Spatial Variations of the Strength of CO₂ Absorption and the Rotational Temperature on Venus(Dissertation_全文)

AUTHOR(S):

Iwasaki, Kyosuke

CITATION:

Iwasaki, Kyosuke. Spatial Variations of the Strength of CO₂ Absorption and the Rotational Temperature on Venus. 京都大学, 1976, 理学博士

ISSUE DATE:

1976-03-23

URL:

<https://doi.org/10.14989/doctor.r2972>

RIGHT:

理
224
1-1

學位申請論文

岩崎恭輔

SPATIAL VARIATIONS OF THE STRENGTH OF CO₂ ABSORPTION
AND THE ROTATIONAL TEMPERATURE ON VENUS

KYOSUKE IWASAKI

KWASAN OBSERVATORY, UNIVERSITY OF KYOTO, KYOTO

Abstract

The CO_2 8689 Å band in the spectrum of Venus was observed with the echelle spectrograph of the coudé focus of the 74-inch reflector at Okayama Astrophysical Observatory in 1973 and 1974 when the phase angle of Venus was near 90° . The dispersion of the spectrum was 2.5 Å/mm. The slits of the spectrograph were placed along the terminator and along the intensity equator. In our method of reduction the spatial variation of the CO_2 absorption is obtained from a single spectrum, so it is not necessary to separate the spatial variation from the temporal variation and the spatial variation corresponds to a smaller range of longitude or latitude than those obtained from previous methods.

The CO_2 absorptions decrease at high latitudes along the terminator and have a maximum on the intensity equator. These spatial variations would be explained theoretically with a homogeneous, isotropic scattering atmosphere.

The spatial variations of the slope of the curve of growth and the rotational temperature were also analyzed. The slope of the curve of growth increases slightly toward high latitudes along the terminator. It seems that the rotational temperature decreases toward high latitudes along the morning terminator but does not show any systematic variation along the evening terminator.

Key words: Venus; Planetary atmosphere; Planetary spectra; CO_2 absorption; Rotational temperature.

1. Introduction

The phase variation of the equivalent width for numerous CO_2 bands was observed by many observers (Kuiper 1952; Chamberlain and Kuiper 1956; Spinrad 1962; Moroz 1968; Gray and Schorn 1968; Gray et al. 1969; Schorn et al. 1969, 1970, 1971; Young et al. 1969, 1970). All of these observations suggest that the equivalent width decreases with increasing phase angle of Venus. This phase variation has been explained by models of a homogeneous, isotropically scattering atmosphere (Chamberlain and Kuiper 1956; Chamberlain and Smith 1970). The observations of Young et al. (1971) and of Young (1972) include the phase angle around inferior conjunction and appear to suggest a decrease in the equivalent width toward small phase angles from the phase angles of $50-80^\circ$. Such an "inverse phase effect" was interpreted by some models (Carleton and Traub 1972; Hunt 1972; Regas et al. 1973; Whitehill and Hansen 1973; Chamberlain 1975).

Spatial Variation of the equivalent width for the CO_2 band was observed by many observers (Kuiper 1952; Belton et al. 1968; Moroz 1971 a, b; Young et al. 1973, 1974; Barker and Perry 1975). Young et al. (1973, 1974) observed spatial and temporal variations of the CO_2 absorption in the spectrum of Venus. Their data indicate a semi-regular 4-day variation of the apparent strength of the CO_2 absorptions. Their data also indicate that there is more CO_2 absorption near the terminator than at the limb, and slightly

more in the southern than in the northern hemisphere. Barker and Perry (1975) observed the spatial variation of the CO_2 line strength for various phase angles and found the polar versus equatorial asymmetry noted previously by Moroz (1971a, b) and the long-term changes, more than one year, in the CO_2 absorption.

In the method of observation and reduction by previous authors, the spatial variation of CO_2 absorption has been obtained by comparing some spectra observed at different dates and times. Therefore it is necessary to separate the spatial variation from the temporal variation. Moreover the obtained longitudinal (or latitudinal) variation corresponds not to a definite latitude (or longitude) but to a fairly wide range of latitude (or longitude). In our method proposed in this paper, the spatial variation of the CO_2 absorption is obtained from a single spectrum, so it is not necessary to separate the spatial variation from the temporal variation and the spatial variation corresponds to a smaller range of longitude or latitude than those obtained by the previous method. In order to obtain the spatial variations of the CO_2 absorption with our method, spectroscopic observations of the CO_2 8689 Å band were made in November, 1973 and in April, 1974. These observing periods were particularly favourable for this purpose, because the intensity variation along the terminator is minimum at the phase angle near 90° . We can measure the latitudinal variation of CO_2 variation along the terminator most realistically in this phase angle. In section 3, the observed spatial variations

of CO_2 absorption are presented. The comparison of this observation with the theoretical variations obtained from the model assuming a homogeneous, isotropically scattering atmosphere are also presented in section 3.

Young et al. (1969) showed in their analysis of the CO_2 8689 Å band that the rotational temperatures do not vary from region to region on the planet. However, Young et al. (1975) recently found evidence for temporal and spatial variations in the rotational temperature. To examine whether the spatial variation of the rotational temperature exist or not, we also study the latitudinal variation of the rotational temperature. In order to determine the rotational temperature, we must know the absorption law, i.e., the slope of the curve of growth. In section 4, we first examine the spatial variation of the slope of the curve of growth. Then the spatial variation of the rotational temperature is examined

2. Observations and Reductions

The observations were carried out with the echelle spectrograph of the coudé focus ($F=54\text{m}$) of the 74-inch reflector at Okayama Astrophysical Observatory. Table 1 gives the basic data for our plates. The first column gives the plate number. The second and third columns are date and time of the observations. The fourth column gives the phase angle of Venus (Sun-Venus-Earth). The fifth

column indicates the position of the slit on the disk of Venus. Position 1 is parallel to the evening terminator near the center of the disk; position 2 is along the intensity equator; position 3 is parallel to the morning terminator near the center of the disk. An image rotator was used to fix the slit position. In our observations, various parts of the slit correspond to those of the disk of Venus. For example, in the case of position 1 and 3, the center of the spectrogram corresponds to the intensity equator, and the both edges of the spectrogram correspond to the polar regions. Spectra were taken on ammonia-hypersensitized Kodak I-N emulsions in September 1973, and ammonia-hypersensitized Kodak IV-N emulsions (Barker 1968) in April 1974. The dispersion on the plate is 2.5 \AA/mm at 8689 \AA . The projected slit width was 20μ . The image of Venus on the slit was contaminated by seeing and by imperfections in guiding. In order to determine the apparatus function on the observing night, the spectrograms of Moon and some bright stars neighboring Venus were also taken just before and just after the exposures for Venus.

The exposed plates were traced in the direction of dispersion in the density mode on a microphotometer. The projected slit height of the spectrometer was 200μ for IV-N plate and 400μ for I-N plate. They correspond to about 12 per cent and about 24 per cent of the diameter of the disk of Venus, respectively. Many tracings were made over various parts of the strip of the spectrogram. In the case of position 1 and 3, we can examine the latitudinal

variation of CO_2 absorption along the terminator. In the case of position 2, we can examine the longitudinal variation in the intensity equator. Figure 1 shows the CO_2 8689 Å band.

To measure the equivalent width, we used the square counting method and the simple method, in which the equivalent width was measured from the product of the central intensity and the $1/e$ half-width. The differences of the values of the equivalent widths obtained by these two methods were within a few per cent. For our simple method the spatial variation of the equivalent width can be divided into the variation of the central intensity and the $1/e$ half-width. In our observations, the $1/e$ half-width does not show any systematic spatial variation. This is expected from the fact that the CO_2 line of Venus is narrow compared to the instrumental width so the apparent line profile of the CO_2 line is the instrumental profile. Thus, the spatial variation of the central intensity corresponds to that of the equivalent width.

To obtain an estimate of the true spatial variation of the central intensity, it is necessary to deconvolve the observed intensity profile with the apparatus function. The estimates of the apparatus function were obtained from the observations of the limb of the Moon and some bright stars neighboring Venus. The intensity profile of a star image, obtained from the spectrogram tracing of the star perpendicular to the direction of dispersion with the projected slit height of 200 μ or 400 μ , was used for the apparatus function of the observing night. The first derivative

of the intensity profile of the limb of the Moon was also used for the apparatus function. These apparatus functions were approximated by Gaussian profile. The obtained half-widths of these Gaussian profiles were less than 2.6 sec of arc. This value is about 11 per cent of the diameter of the disk of Venus. Observed intensity profiles were deconvolved with these Gaussian profiles. The results indicated that the observed and derived true intensity profiles agree within the noise level of data in the spatial range in which we measured the variation of central intensity. Thus we use the observed intensity profiles for our analyses. It is safely considered that the profile of the apparatus function does not change in every direction. Then the intensity profile we obtained is the averaged one within the range of apparatus function in the direction perpendicular to that of the slit.

3. Spatial Variation of CO_2 Absorption

3.1. Observed Variation

We have measured the central intensities of the P(8)-P(28) lines. In the case of the slit position along the terminator, the relative value of the central intensity of each P(J) line, normalized to that of the intensity equator, is measured on each

position of the disk of Venus. In the case of the slit position along the intensity equator, the central intensity of each P(J) line is referred to that of the position where the maximum value occurs. The relative CO₂ line strength of each position is obtained by averaging these normalized central intensities of the P(J) lines. The errors in measuring central intensity are largely due to uncertainties in estimating the continuum level. In order to estimate these uncertainties, we measured the central intensities of eight solar lines located near the band. For the solar line, the central intensity of each solar line is normalized to the mean value of the central intensities of various positions. As the central intensities of solar lines do not vary over the disk of Venus, the standard deviation of the central intensity of the solar line would indicate the amount of errors in our measuring process, and therefore we assume this value would be same for the case of CO₂ lines. The relative line strengths of CO₂ line and of solar line, and their standard deviations are given in table 2. Figures 2(a), 2(b), and 2(c) show the latitudinal variation of the relative line strengths of CO₂ line and of solar line along the terminator. In these figures we can see that the relative CO₂ line strength decreases toward the high latitude along the terminator, whereas that of solar line does not show any systematic variation. The longitudinal variation of the relative line strength along the intensity equator is illustrated in figure 3. It is obvious in this figure that the relative CO₂ line strength has a maximum, whereas the relative line strength of solar line is

nearly constant.

3.2. Comparison with the Theoretical Variation

To compare the observed variation with the theoretical one, we consider a model of the homogeneous, isotropically scattering atmosphere. The adequacy of the homogeneous model for the phase variation is recently demonstrated by Kawabata and Hansen (1975). They have computed the polarization of reflected sunlight for a homogeneous model atmosphere and for a reflecting layer model, and compared the calculations with observations of Coffeen and Gehrels (1969) and of Dollfus and Coffeen (1970). They concluded that the homogeneous model atmosphere is in better agreement with the observations than the reflecting layer model is. In the homogeneous, isotropically scattering atmosphere, the equivalent width of a CO_2 line is proportional to $(\mu_0 + \mu)$, where $\arccos \mu_0$, and $\arccos \mu$ are the angle of incidence, and of emergence (Chamberlain 1965, 1970; Belton et al. 1968). In our observation, the spatial variation of the central intensity corresponds to that of the equivalent width as discussed in section 2. So we can compare the theoretical variation of the equivalent width with the observed variation of the central intensity. The theoretical variation is also shown in figures 2(a), 2(b), 2(c), and 3. From figures 2(a), 2(b), and 2(c), it is obvious that our observed

variation and the theoretical one have similar tendency, i.e., equivalent width decreases toward the high latitude. Along the intensity equator theoretical variation has a maximum at the position of $r/R=0.7$ (figure 3). This maximum also appears in our observed variation near the position indicated by the theoretical model. We can say that our observed variations would show similar trend to the theoretical ones estimated from a model of the homogeneous, isotropically scattering atmosphere, although real atmosphere is inhomogeneous and the scattering is anisotropic in some degree.

4. Spatial Variations of the Slope of the Curve of Growth and of the Rotational Temperature

The intensity of a rotational line is proportional to the product of the number of molecules in the lower rotational energy state and the square of the matrix element for the rotational transition. For the P branch ($\Delta J = -1$) the square of the matrix element is proportional to the rotational quantum number (J) (Chamberlain 1965). Then the rotational line intensity of the P branch is given by

$$S = \frac{S_{\text{band}} \cdot J}{Q_{\text{rot}}} \exp \left[- \frac{hc B_v}{k T_{\text{rot}}} J(J+1) \right], \quad (1)$$

where S_{band} is the band intensity, T_{rot} is the rotational temperature to be determined, B_v is the rotational constant for the lower vibrational state, h is the Planck's constant, k is the Boltzmann constant, and $Q_{\text{rot}} = kT_{\text{rot}}/hcB_v$ is the rotational partition function (Herzberg 1950). Chamberlain and Kuiper (1956), working with the CO_2 bands at 8689 and 7820 Å, found that absorption lines formed in a scattering atmosphere followed a square-root absorption law. Belton (1968) has developed a theory of curve of growth in a semi-infinite, homogeneous, isotropically scattering atmosphere and showed that the band at 8689 Å lay on a roughly square-root portion of the curve of growth. Young et al. (1969) also found a square-root absorption law in their analysis of the CO_2 8689 Å band. To see if the square-root absorption law is valid for every position on the disk of Venus, we calculated the slope of the curve of growth as has previously done by Young et al. (1969). If we assume that the curve of growth can be locally approximated by a straight line of slope, b , the relation between the equivalent width of a line, W , and the line intensity, S , is given by

$$W \propto S^b. \quad (2)$$

Substitution of equation (1) in equation (2) gives

$$\ln \frac{W}{Jb} = \ln W_0 - \frac{0.5614 J(J+1)}{T_{\text{rot}}} b. \quad (3)$$

If we know the value of b (i.e., the absorption law), and plot

$\ln W/J^b$ versus $J(J+1)$, the rotational temperature can be found from a linear least-squares fit to the data. The slope of the curve of growth and the rotational temperature are computed by an iterative procedure. First, relative intensities are calculated for an assumed rotational temperature, then the slope, b , of the curve of growth is obtained from a linear least-squares solution of equation (2). Using the calculated value of b , the rotational temperature is recalculated from equation (3). For this rotational temperature, the relative intensities are recalculated. In this way iterative procedure is repeated until the rotational temperature exhibits no further change. The results of these calculations are given in table 2 and shown in figures 4(a), 4(b), and 4(c). These figures show that the slope, b , of the curve of growth increases slightly at the high latitude along the terminator. In figure 4(b) it seems that the rotational temperature decreases toward the high latitude along the morning terminator. Figure 4(a) also shows the variation along the morning terminator. In some regions ($r/R=0.29S$, $0.06S$, and $0.06N$), the slope, b , is slightly smaller than 0.5, but we should assume the slope equals to 0.5 in these regions. Then the rotational temperatures increase and the variation of the rotational temperature shows the polar cooling. In figure 3(c), which shows the variation along the evening terminator, we see that the rotational temperature does not vary systematically.

5. Discussion

Spatial variation of the equivalent width for the CO_2 band was discovered by Kuiper (1952). He reported that the patches of CO_2 absorption may correspond to the ultra-violet cloud features (Murray et al. 1974). Belton et al. (1968) made a number of observations of the CO_2 8689 Å band strengths for the equator- and the polar-regions. However, they reported that their visual inspection of the data suggested no change at all. Moroz (1971a, b) observed the spectrum near the CO_2 1.6 μ band at various parts of the crescent near inferior conjunction. He found that the equivalent bandwidths were several times greater at the southern cusp than at the intensity equator and/or than at the northern cusp. He explained this strong asymmetry by the geometry of the observations, i.e., the southern cusp is near the planetary pole, while the northern cusp is in the tropical and temperate zones. In his geometry of the observations he considered that the direction of the north pole of the planet was coincident with that of celestial north, so the equatorial plane of Venus was inclined about 30° from the intensity equator of Venus in his observing period. However, the pole of Venus is very nearly perpendicular to the orbital plane (Carpenter 1964; Goldstein 1964, 1970) and the orbit of Venus is inclined 3°4 to the ecliptic, so the equator of Venus is nearly coincident with the intensity equator. In this geometry we still have strong asymmetry in the observations of Moroz. Hunt and Schorn (1971) pointed out that it is impossible

to draw the conclusion obtained by Moroz from his observations. The date of the observation of the Moon which was used as a calibration was different from that of Venus in his observations. They pointed out that infrared observations of low dispersion, such as those made by Moroz, must be carried out at equal altitudes and as close together as possible in time, so any comparison made of the Venus spectra with those of the Moon is meaningless.

The latitudinal variation of the central intensity of CO_2 lines has been studied by Young et al. (1974) and by Barker and Perry (1975). Young et al. (1974) report that there is slightly ($\sim 3\%$) larger CO_2 absorption in the southern hemisphere during the observational period of September 1972 when the phase angle, $\bar{\alpha}$, is $78-73^\circ$. Barker and Perry (1975) observed the relative CO_2 line strength in various phase angles. They show that the southern hemisphere has slightly ($\sim 3\%$) larger CO_2 absorption when averaged over the observational period of September 1972 ($\bar{\alpha}=75-70^\circ$). On the other hand, they show that intensity equatorial region has slightly larger CO_2 absorption in the period of August 1973 ($\bar{\alpha}=47-54^\circ$), October 1973 ($\bar{\alpha}=76-79^\circ$), and December 1973 ($\bar{\alpha}=109-113^\circ$). In our observational period of November 1973 ($\bar{\alpha}=87^\circ$) and April 1974 ($\bar{\alpha}=90-87^\circ$), the CO_2 absorption decreases toward high latitudes along the terminator. This sense of the spatial variation agrees with the results of Barker and Perry (1975) in their August 1973, October 1973, and December 1973 data, although we are sampling a smaller longitudinal region along the terminator.

Young et al. (1974) also examine the longitudinal variation and show that there is more CO_2 absorption in the terminator side than the limb side of the disk of Venus during the period of time in September 1972 ($\lambda=79-73^\circ$). Barker and Perry (1975) report that limb has slightly ($\sim 3\%$) larger CO_2 line strength than the terminator during the period of October 1973 ($\lambda=76-79^\circ$), whereas this asymmetry is opposite to that observed during December 1973 ($\lambda=109-113^\circ$). In our observation, the longitudinal variation along the intensity equator of the CO_2 absorption has a maximum at the position of $r/R=0.7$. The sense of this variation agrees with the terminator-limb asymmetry obtained by Barker and Perry (1975) in October 1973, although we are sampling a smaller latitudinal region along the intensity equator.

Both of our longitudinal and latitudinal variations show $(\mu+\mu_0)$ dependency. This dependency would be expected from a model of the homogeneous, isotropically scattering atmosphere. On the other hand, the simple reflecting layer model, in which the CO_2 lines are supposedly formed in clear atmosphere above the clouds, predicts spatial variations which are contrary to our observation. Our longitudinal variation in which the CO_2 absorption decreases toward the terminator side is coincident with the phase variation of the CO_2 absorption in which the CO_2 absorption decreases toward inferior conjunction (Young et al. 1971; Young 1972), since we see only the terminator region at inferior conjunction. A horizontally homogeneous atmosphere which is indicated by our observation,

is also expected from the photochemically produced clouds (Prinn 1971, 1973), because the height of the cloud top is not to vary over the disk of Venus in their cloud model. The observed variation of CE-346 plate shows a depression near the southern mid-latitude and that of CE-329 plate shows that there is more CO_2 absorption in both hemispheres than the value indicated by the theoretical model. These deviations from the theoretical model may be related to relatively small horizontal inhomogeneity in the atmosphere of Venus.

For the CO_2 8689 Å band, the slope, b , of the curve of growth has been considered to be nearly 0.5. Recently Schorn et al. (1975) reported the results of observations made during 1968 and 1969. In their observational period, the phase angles of Venus varied from 10° to 126° . We can examine the phase variation of the slope, b , of the curve of growth from their data. This phase variation is shown in figure 5. From this figure we can see that the slopes for phase angles larger than 100° are slightly higher than those for phase angles smaller than 100° . The sense of this phase variation is coincident with that of our spatial variation in which the slope increases toward high latitudes along the terminator. These variations of the slope of the curve of growth with μ and μ_0 can be explained theoretically by Belton (1968) and by Uesugi and Irvine (1970). They showed that the slope increases as μ (or μ_0) decreases in the model of a semi-infinite, homogeneous, isotropic scattering atmosphere.

A spatial variation in the rotational temperature for the CO_2 7820 A band was found by Young et al. (1975). They found that the average temperature at the equator, determined from a curve of growth analysis, is slightly higher than at the polar region. It seems that the polar cooling along the morning terminator appears in the case of CE-346 and -338. In the case of CE-329, observed along the evening terminator, the rotational temperature appears not to show polar cooling. Our results agree in the sense of variation with the polar cooling found by Ingersoll and Orton (1974). They analyzed the high-resolution maps of the brightness temperatures of Venus in the 8-14 μ wavelength region obtained by Murray et al. (1963) and Westphal et al. (1965) and found that solar associated flux function show the existence of polar cooling and the magnitude of the polar cooling is much greater near the morning terminator than the evening terminator.

The author wishes to express his sincere thanks to Professor S. Miyamoto, Director of the Kwasan and Hida Observatories, and Dr. A. Hattori for their encouragement and valuable advices. He also would like to express his sincere gratitude to Dr. A. Uesugi for reading through the manuscript and for his guidance during the course of the investigation. It is a pleasure for the author to express his thanks to Drs. W. M. Irvine and S. Saito for reading through the manuscript and supplying many stimulating

suggestions. He also sincerely appreciate to the helpful suggestions and encouragement offered by Drs. M. J. S. Belton, J. Kubota, and L. G. Young. He is grateful to the staff of the Okayama Astrophysical Observatory for their kind assistance in the observations. The computations were carried out on a TOSBAC-3400 at the Research Institute for Mathematical Sciences, University of Kyoto. |

References

- Barker, E. S., 1968, *J. Opt. Soc. Amer.*, 58, 1378.
- Barker, E. S., and Perry, M. A. 1975, *Icarus*, 25, 282.
- Belton, M. J. S. 1968, *J. Atmos. Sci.*, 25, 596.
- Belton, M. J. S., Hunten, D. M., and Goody, R. M. 1968, in
The Atmospheres of Venus and Mars, ed. John C. Brandt
 and M. B. McElroy (Gordon & Breach, New York), pp. 69-97.
- Carleton, N. P., and Traub, W. A. 1972, *Bulletin of the
 American Astronomical Society*, 4, 362.
- Carpenter, R. L. 1964, *Astron. J.*, 69, 2.
- Chamberlain, J. W. 1965, *Astrophys. J.*, 141, 1184.
- Chamberlain, J. W. 1970, *Astrophys. J.*, 159, 137.
- Chamberlain, J. W. 1975, *Astrophys. J.*, 195, 815.
- Chamberlain, J. W., and Kuiper, G. P. 1956, *Astrophys. J.*,
 124, 399.
- Chamberlain, J. W., and Smith, G. R. 1970, *Astrophys. J.*,
 160, 755.
- Coffeen, D. L., and Gehrels, T. 1969, *Astron. J.*, 74, 433.
- Dollfus, A., and Coffeen, D. L. 1970, *Astron. Astrophys.*,
 8, 251.
- Goldstein, R. M. 1964, *Astron. J.*, 69, 2.
- Goldstein, R. M. 1970, *Radio Science*, 5, 391.
- Gray, L. D., and Schorn, R. A. 1968, *Icarus*, 8, 409.
- Gray, L. D., Schorn, R. A., and Barker, E. S. 1969, *Applied
 Optics*, 8, 2087.

- Herzberg, G. 1950, in *Molecular Spectra and Molecular Structure, Spectra of Diatomic Molecules*, (D. Van Nostrand Company, New York), p. 125.
- Hunt, G.E. 1972, *J. Quant. Spectrosc. Radiat. Transfer*, 12, 405.
- Hunt, G. E., and Schorn, R. A. J. 1971, *Nature Physical Science*, 233, 39.
- Ingersoll, A. P., and Orton, G. S. 1974, *Icarus*, 21, 121.
- Irvine, W. M., Simon, T., Menzel, D. H., Charon, J., Lecomte, G., Griboval, P., and Young, A. T. 1968a, *Astron. J.*, 73, 251.
- Irvine, W. M., Simon, T., Menzel, D. H., Pikoos, C., and Young, A. T. 1968b, *Astron. J.*, 73, 807.
- Kawabata, K., and Hansen, J. E. 1975, *J. Atmos. Sci.*, 32, 1133.
- Kuiper, G. P. 1952, in *The Atmospheres of the Earth and Planets*, ed.G. P. Kuiper, (University of Chicago Press, Chicago), p. 370.
- Moroz, V. I. 1968, *Soviet Astron.*, 11, 653.
- Moroz, V. I. 1971a, *Nature Physical Science*, 231, 36.
- Moroz, V. I. 1971b, *Soviet Astron.*, 15, 448.
- Murray, B. C., Belton, M. J. S., Danielson, G. E., Davies, M. E., Gault, D., Hapke, B., O'Leary, B., Strom, R., Suomi, V., and Trask, N. 1974, *Science*, 183, 1307.
- Murray, B. C., Wildey, R. L., and Westphal, J. A. 1963, *J. Geophys. res.*, 68, 4813.

- Prinn, R. G. 1971, *J. Atmos. Sci.*, 28, 1058.
- Prinn, R. G. 1973, *Bulletin of the American Astronomical Society*, 5, 300.
- Regas, J. L., Boese, R. W., Giver, L. P., and Miller, J. H. 1973, *J. Quant. Spectrosc. Radiat. Transfer*, 13, 461.
- Schorn, R. A., Gray, L. D., and Barker, E. S. 1969, *Icarus*, 10, 241.
- Schorn, R. A. J., Wozczyk, A., and Gray Young, L. D. 1975, *Icarus*, 25, 64.
- Schorn, R. A., Young, L. G., and Barker, E. S. 1970, *Icarus*, 12, 391.
- Schorn, R. A., Young, L. G., and Barker, E. S. 1971, *Icarus*, 14, 21.
- Spinrad, H. 1962, *Publ. Astron. Soc. Pacific*, 74, 187.
- Uesugi, A., and Irvine, W. M. 1970, *Astrophys. J.*, 161, 243.
- Westphal, J. A., Wildey, R. L., and Murray, B. C. 1965, *Astrophys. J.*, 142, 799.
- Whitehill, L. P., and Hansen, J. E. 1973, *Icarus*, 20, 146.
- Young, A. T., Wozczyk, A., and Young, L. G. 1974, *Acta Astronomica*, 24, 55.
- Young, L. G. 1969, *Icarus*, 11, 66.
- Young, L. D. G. 1972, *Icarus*, 17, 632.
- Young, L. D. G., Schorn, R. A., and Barker, E. S. 1970, *Icarus*, 13, 58.
- Young, L. D. G., Schorn, R. A., Barker, E. S., and MacFarlane, M. 1969, *Icarus*, 11, 390.

- Young, L. D. G., Schorn, R. A. J., Barker, E. S., and Woszczyk, A. 1971, *Acta Astronomica*, 21, 329.
- Young, L. G., Young, A. T., Young, J. W., and Bergstralh, J. T. 1973, *Astrophys. J. Letters*, 181, L5.
- Young, L. D. G., Young, A. T., and Woszczyk, A. 1975, *Icarus*, 25, 239.

Table 1. Observations of the CO₂ 8689 Å band of
Venus

Plate	Date	Time, U.T.	Phase angle	Slit orientation
CE-329	11/07/73	9 ^h 06 ^m - 9 ^h 57 ^m	87°	1
CE-338	4/05/74	19 ^h 59 ^m - 20 ^h 53 ^m	90°	3
CE-343	4/09/74	21 ^h 03 ^m - 21 ^h 10 ^m	87°	2
CE-346	4/10/74	19 ^h 45 ^m - 20 ^h 35 ^m	87°	3

Table 2. Spatial variations of relative line strength
of CO₂ line and of solar line.

Plate	Position r/R_{venus}	Relative line strength	
		CO ₂ line	solar line
CE-338	0.63S	0.79 \pm 0.04	0.99 \pm 0.06
	0.51S	0.85 \pm 0.04	1.00 \pm 0.03
	0.40S	0.91 \pm 0.04	1.01 \pm 0.04
	0.29S	0.95 \pm 0.04	1.01 \pm 0.02
	0.17S	0.98 \pm 0.02	1.01 \pm 0.03
	0.06S	1.00 \pm 0.01	1.00 \pm 0.04
	0.06N	1.00 \pm 0.02	1.00 \pm 0.03
	0.17N	0.99 \pm 0.02	1.01 \pm 0.04
	0.29N	0.97 \pm 0.02	1.00 \pm 0.03
	0.40N	0.93 \pm 0.03	1.00 \pm 0.03
	0.51N	0.88 \pm 0.03	0.98 \pm 0.03
CE-346	0.61S	0.85 \pm 0.04	1.00 \pm 0.03
	0.48S	0.86 \pm 0.04	1.01 \pm 0.03
	0.36S	0.89 \pm 0.03	1.00 \pm 0.04
	0.24S	0.82 \pm 0.05	0.99 \pm 0.04
	0.12S	0.94 \pm 0.04	0.98 \pm 0.03
	0.00	1.00 \pm -	1.02 \pm 0.02
	0.12N	1.01 \pm 0.02	1.00 \pm 0.04

Table 2. (Continued)

Plate	Position	Relative line strength	
	r/R_{venus}	CO ₂ line	solar line
CE-346	0.24N	0.98 \pm 0.05	0.99 \pm 0.03
	0.36N	0.95 \pm 0.05	1.02 \pm 0.03
	0.48N	0.90 \pm 0.07	1.01 \pm 0.05
	0.61N	0.86 \pm 0.09	0.98 \pm 0.03
CE-329	0.70S	0.75 \pm 0.05	0.90 \pm 0.04
	0.47S	0.95 \pm 0.06	1.02 \pm 0.06
	0.23S	0.98 \pm 0.05	1.00 \pm 0.06
	0.00	1.00 -	1.03 \pm 0.03
	0.23N	0.97 \pm 0.03	1.02 \pm 0.06
	0.47N	0.97 \pm 0.06	1.04 \pm 0.03
	0.70N	0.78 \pm 0.06	0.99 \pm 0.05
CE-343	0.36E	0.93 \pm 0.04	1.00 \pm 0.06
	0.48E	0.97 \pm 0.05	1.01 \pm 0.07
	0.60E	1.00 \pm 0.03	1.00 \pm 0.03
	0.72E	1.00 -	1.01 \pm 0.04
	0.84E	0.96 \pm 0.04	0.99 \pm 0.06
	0.96E	0.88 \pm 0.05	0.99 \pm 0.05

Table 3. Rotational temperature and slope of the curve of growth for the curve of growth absorption law.

Plate	Position r/R_{venus}	Slope of curve of growth b	Rotational temperature $T(b)$ K
CE-338	0.63S	0.537 ± 0.016	222^{218}_{226}
	0.51S	0.696 ± 0.073	249^{237}_{262}
	0.40S	0.593 ± 0.060	249^{238}_{261}
	0.29S	0.410 ± 0.031	250^{242}_{260}
	0.17S	0.564 ± 0.068	269^{256}_{284}
	0.06S	0.482 ± 0.038	250^{241}_{259}
	0.06N	0.410 ± 0.034	251^{241}_{261}
	0.17N	0.540 ± 0.044	269^{260}_{279}
	0.29N	0.553 ± 0.049	250^{240}_{260}
	0.40N	0.574 ± 0.049	250^{240}_{260}
	0.51N	0.630 ± 0.042	250^{241}_{259}
CE-346	0.61S	0.620 ± 0.034	251^{244}_{260}
	0.48S	0.494 ± 0.042	253^{241}_{266}
	0.36S	0.472 ± 0.039	256^{244}_{270}
	0.24S	0.498 ± 0.034	270^{260}_{282}
	0.12S	0.496 ± 0.028	269^{260}_{279}
	0.00	0.492 ± 0.034	270^{259}_{281}
	0.12N	0.538 ± 0.033	267^{258}_{277}

Table 3. (Continued)

Plate	Position r/R_{venus}	Slope of curve of growth b	Rotational temperature $T(b)$ K
CE-346	0.24N	0.495 ± 0.060	254 ²³⁷ 274
	0.36N	0.541 ± 0.037	276 ²⁶⁵ 287
	0.48N	0.617 ± 0.067	257 ²⁴² 274
	0.61N	0.607 ± 0.044	248 ²³⁸ 259
CE-329	0.70S	0.741 ± 0.063	238 ²²⁸ 249
	0.47S	0.663 ± 0.051	272 ²⁵⁸ 287
	0.23S	0.556 ± 0.037	250 ²⁴¹ 260
	0.00	0.545 ± 0.037	239 ²²⁹ 248
	0.23N	0.540 ± 0.040	254 ²⁴⁴ 266
	0.47N	0.553 ± 0.046	241 ²²⁹ 253
	0.70N	0.565 ± 0.029	254 ²⁴⁵ 263

Figure Captions

Figure 1. Reproduction of section of echelle spectrogram of Venus on April 10, 1974 (phase angle 87°), showing the CO_2 8689 Å band. The spectrograph slit is placed parallel to the terminator near the center of the disk of Venus. The positions of the R- and P-branch lines are indicated. Original dispersion 2.5 Å/mm on IV-N⁺ emulsion.

Figure 2. Spatial variations of relative line strength of CO_2 line and of solar line along the terminator. Observational variation of CO_2 line is represented by open circles. Theoretical variation obtained from a model of the homogeneous, isotropically scattering atmosphere is shown by the solid line. Filled circles indicate the variation of solar line. Error bars denote the standard deviation.

Figure 3. Spatial variations of relative line strength of CO_2 line and of solar line along the intensity equator. Symbols are the same as in figure 1. S.S.P., subsolar point.

Figure 4. Spatial variations of the slope of the curve of growth and of the rotational temperature, found assuming a curve of growth absorption law, along the terminator. Filled circles indicate the slopes of the curve of growth. Open circles represent the rotational temperatures. Error bars denote the standard deviation.

Figure 5. Slope of the curve of growth as a function of Venus phase angle. The data are taken from Schorn et al. (1975).

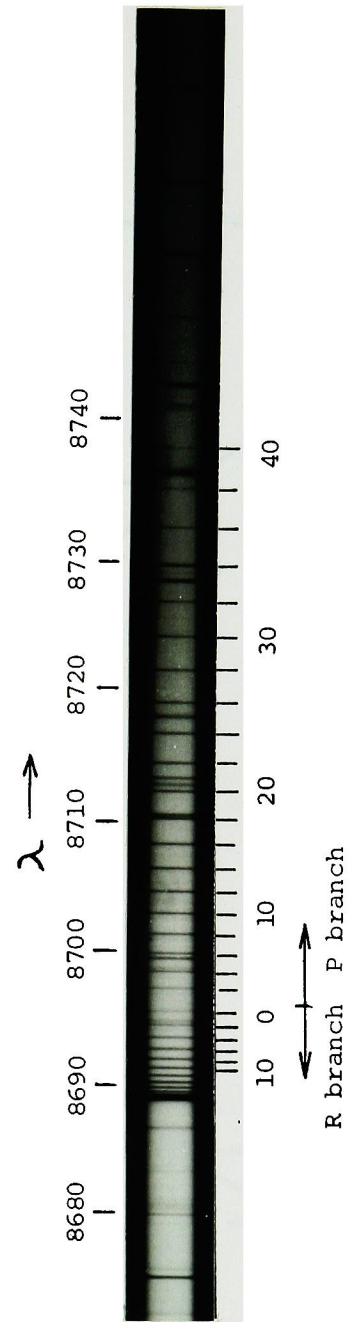


Fig. 1.

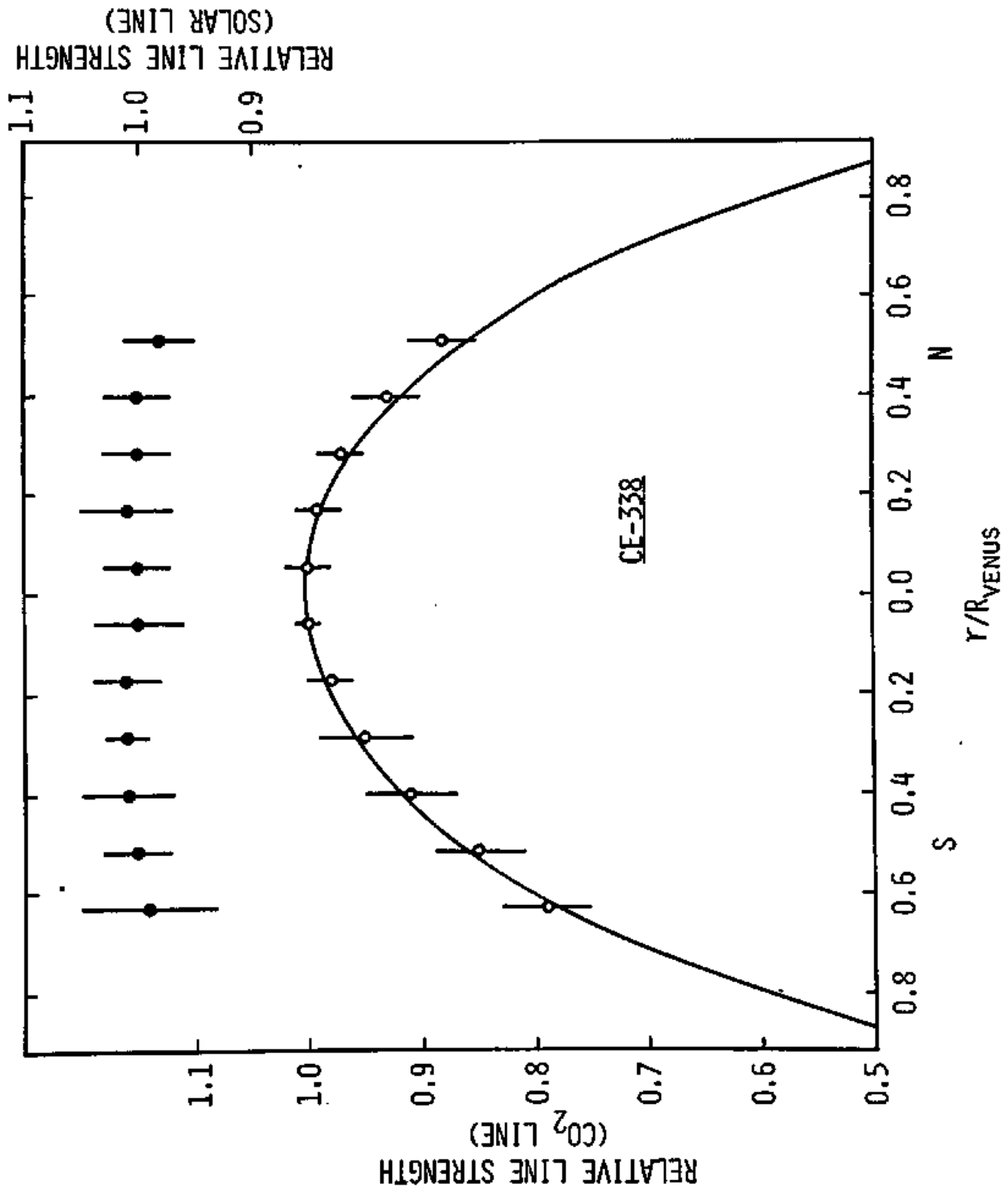


Fig. 2.(a)

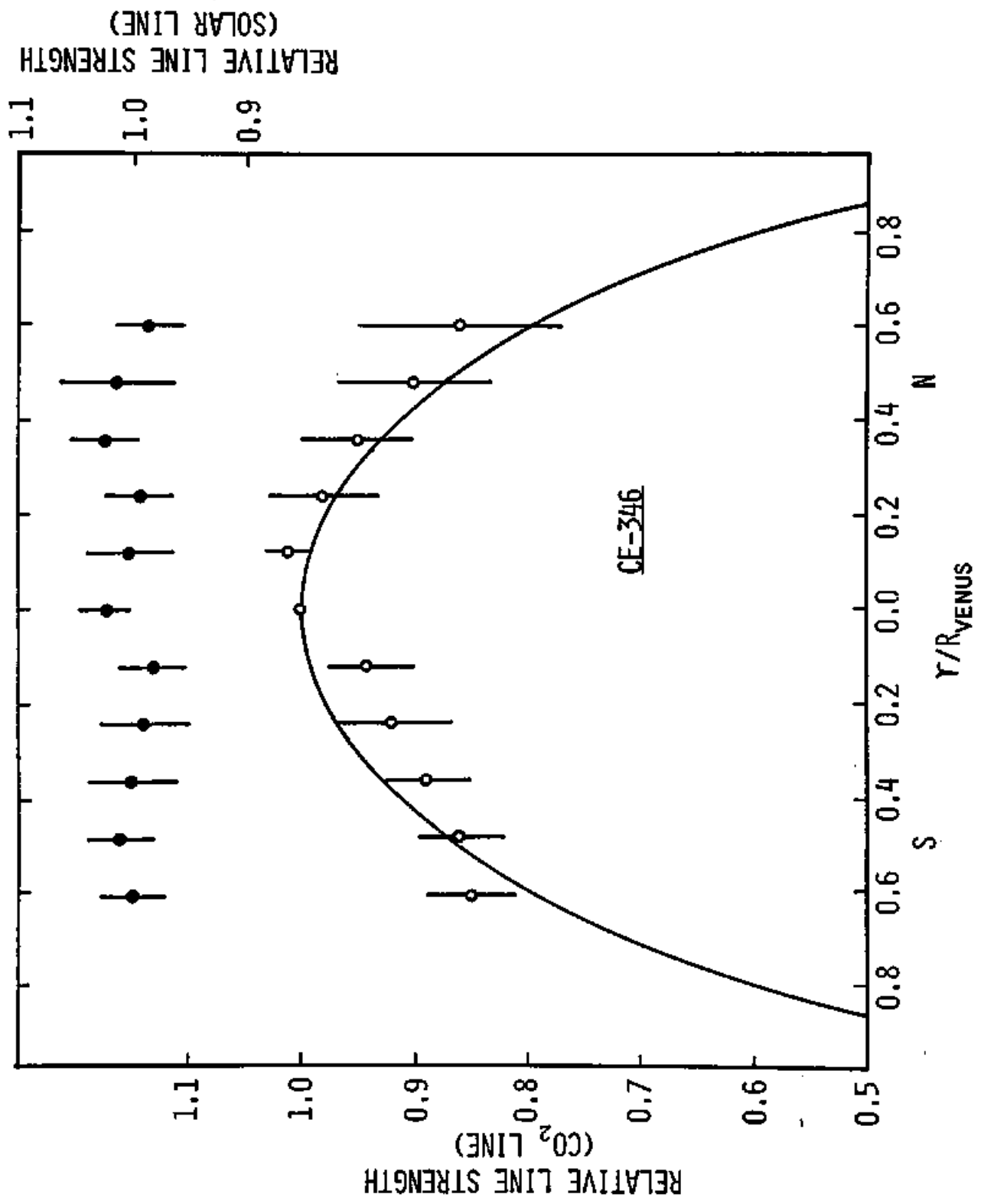


Fig. 2.(b)

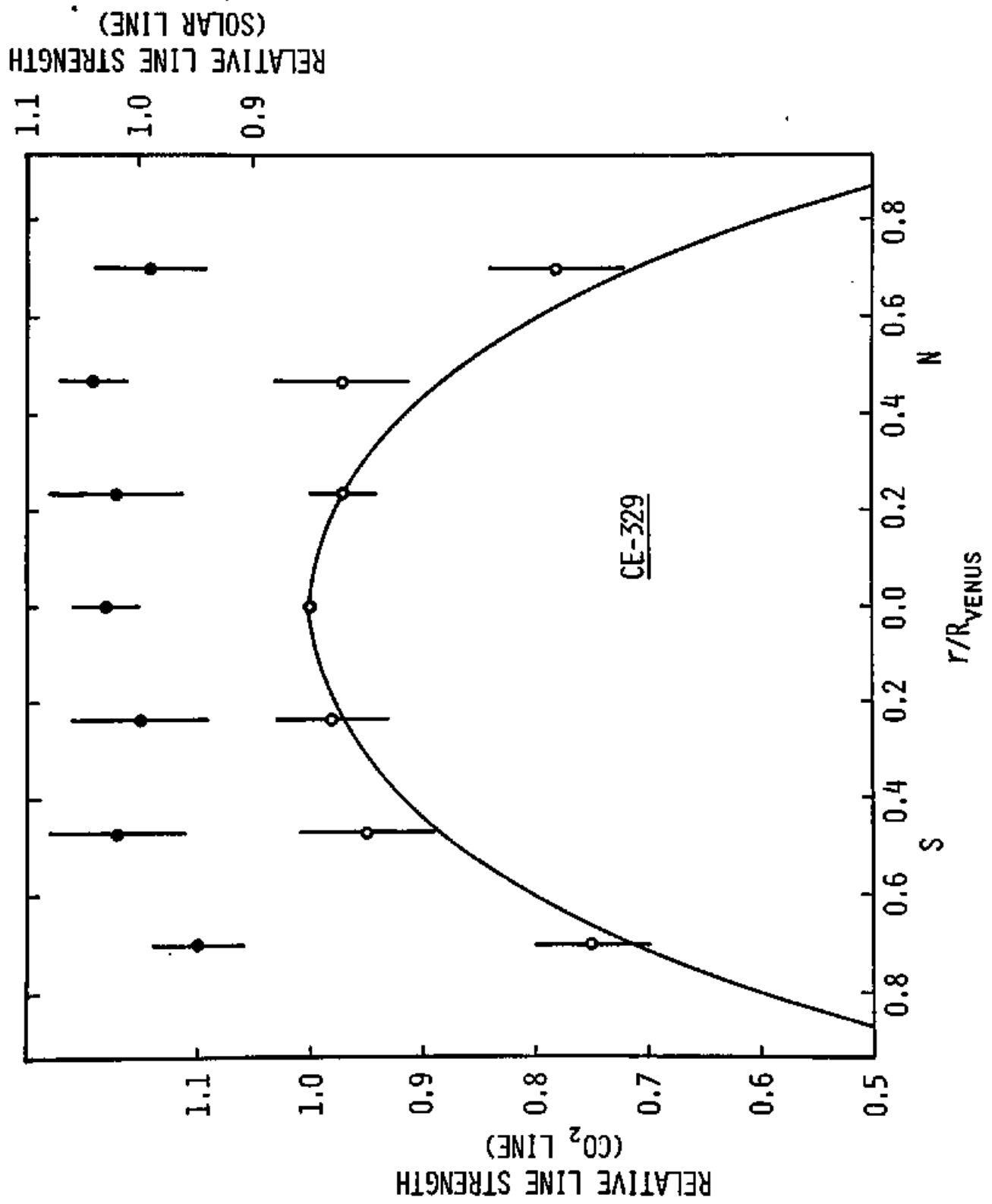


Fig. 2.(c)

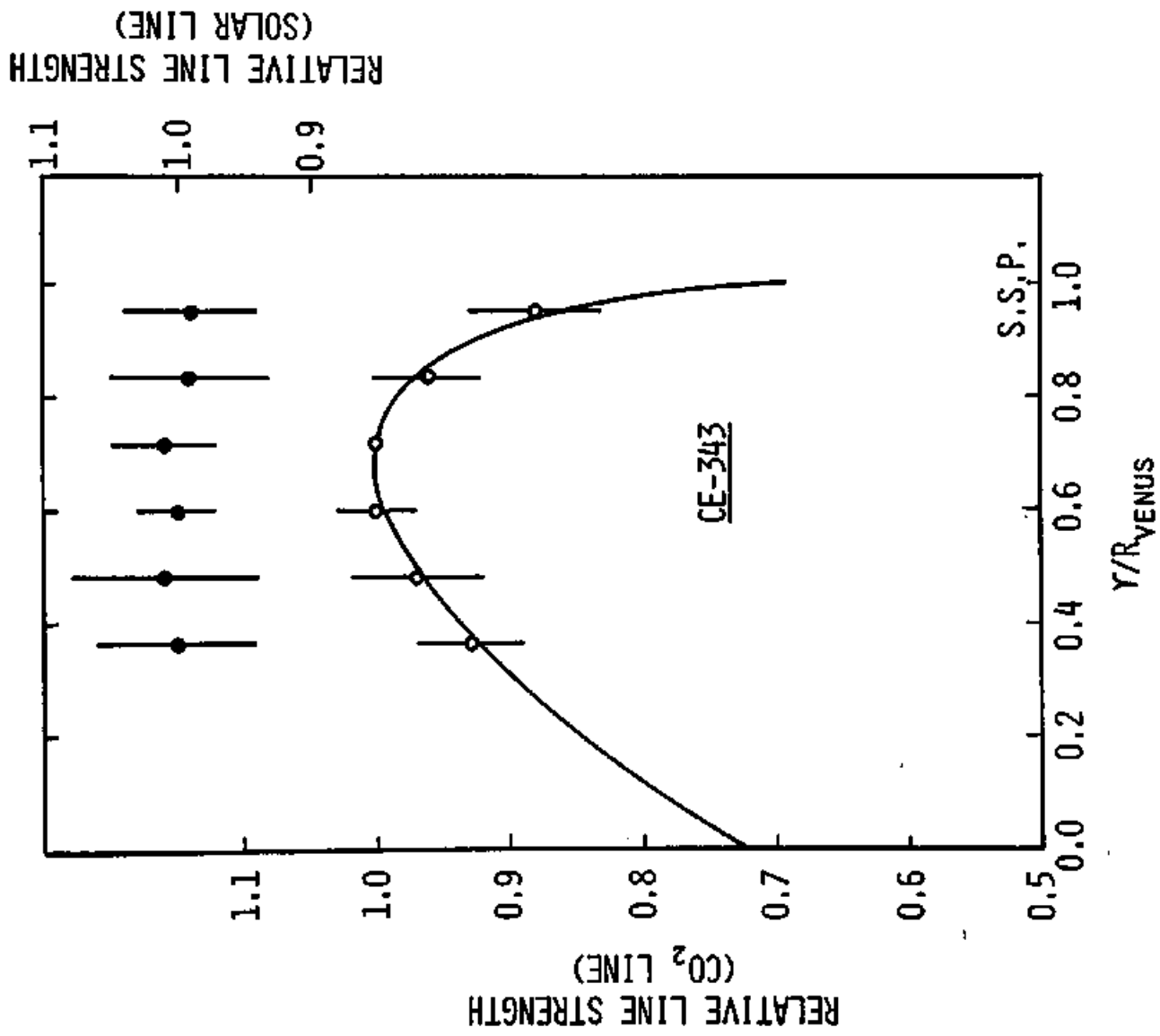


Fig. 3.

SLOPE OF CURVE OF GROWTH

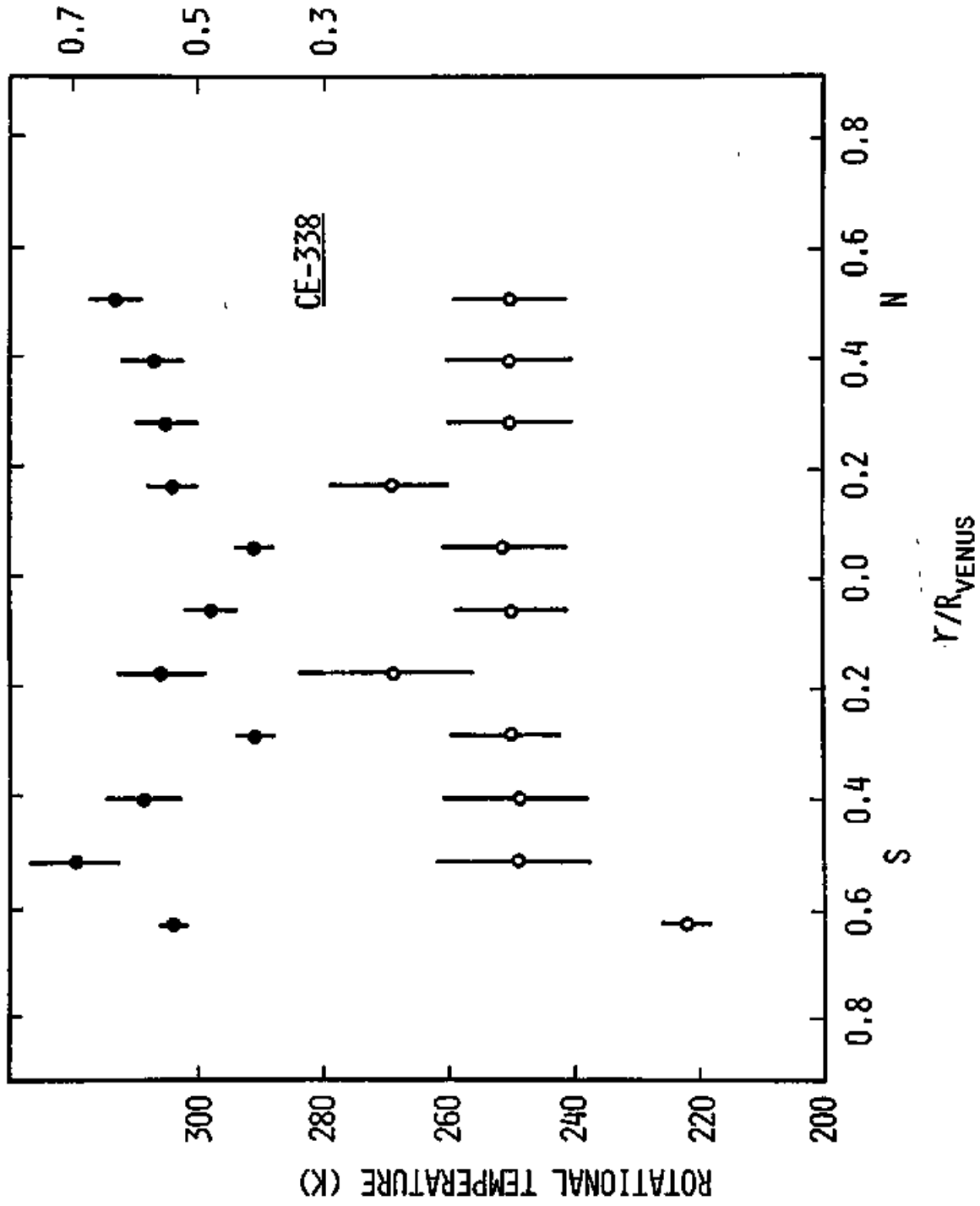


Fig. 4.(a)

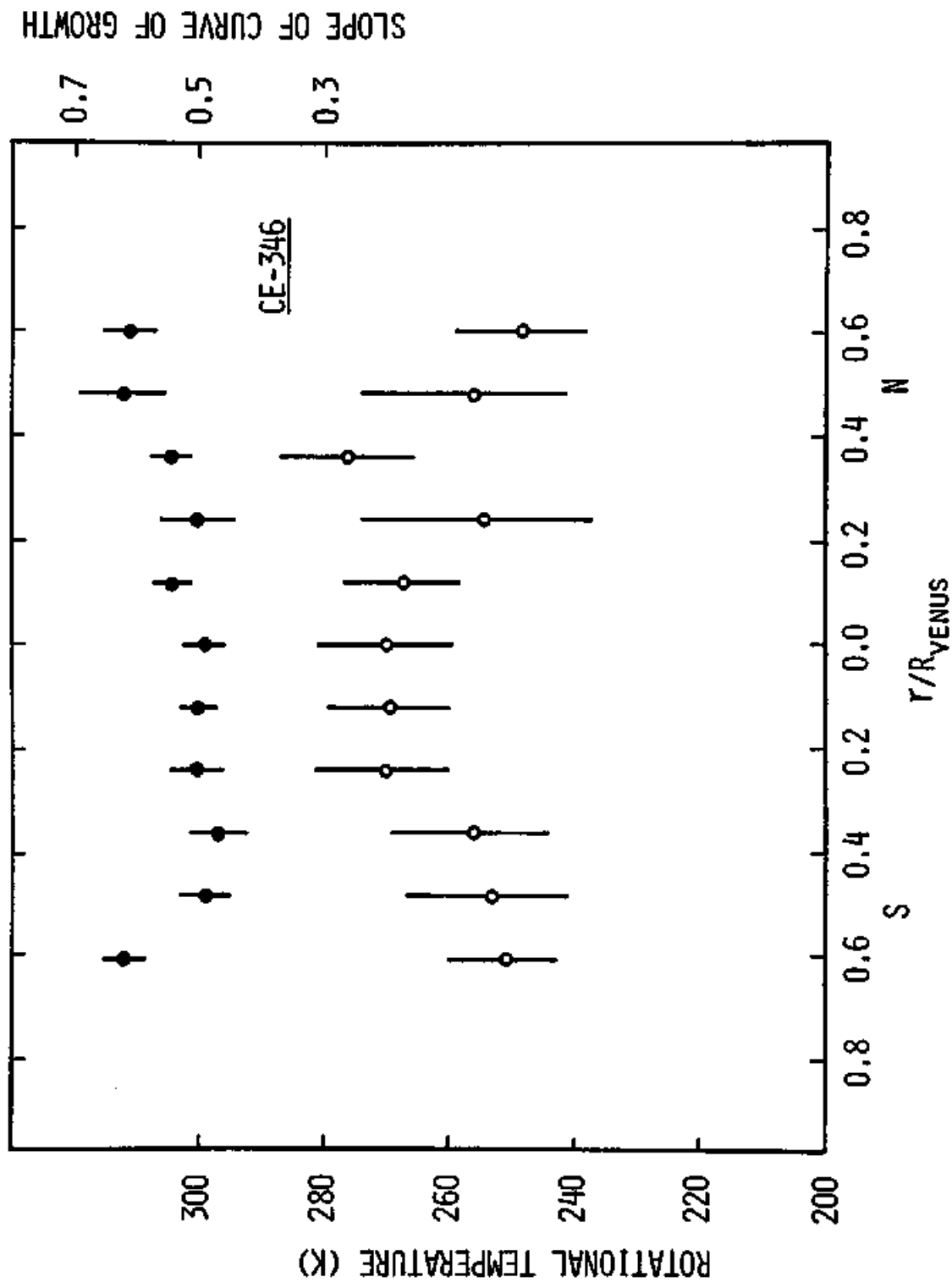


Fig. 4.(b)

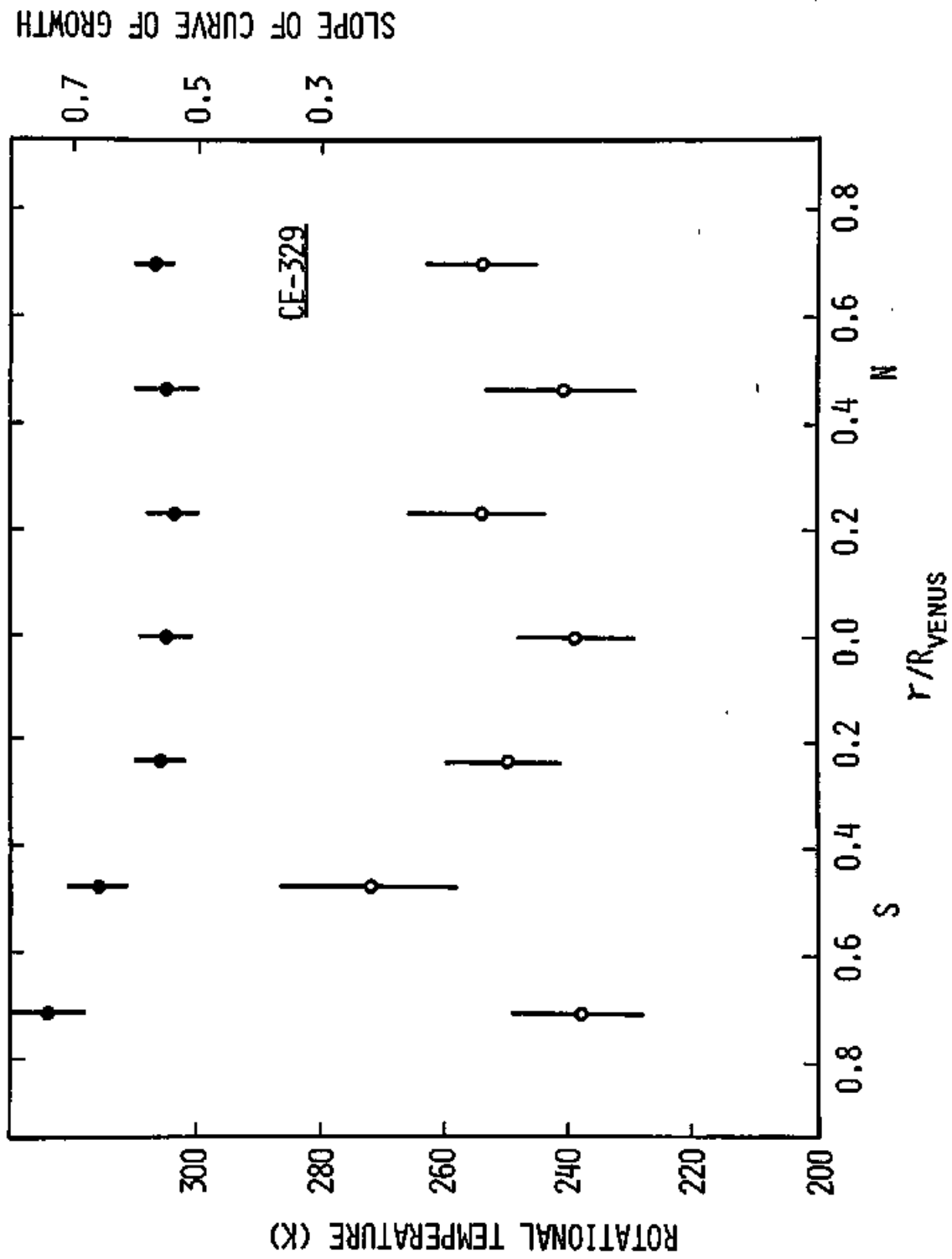


Fig. 4.(c)

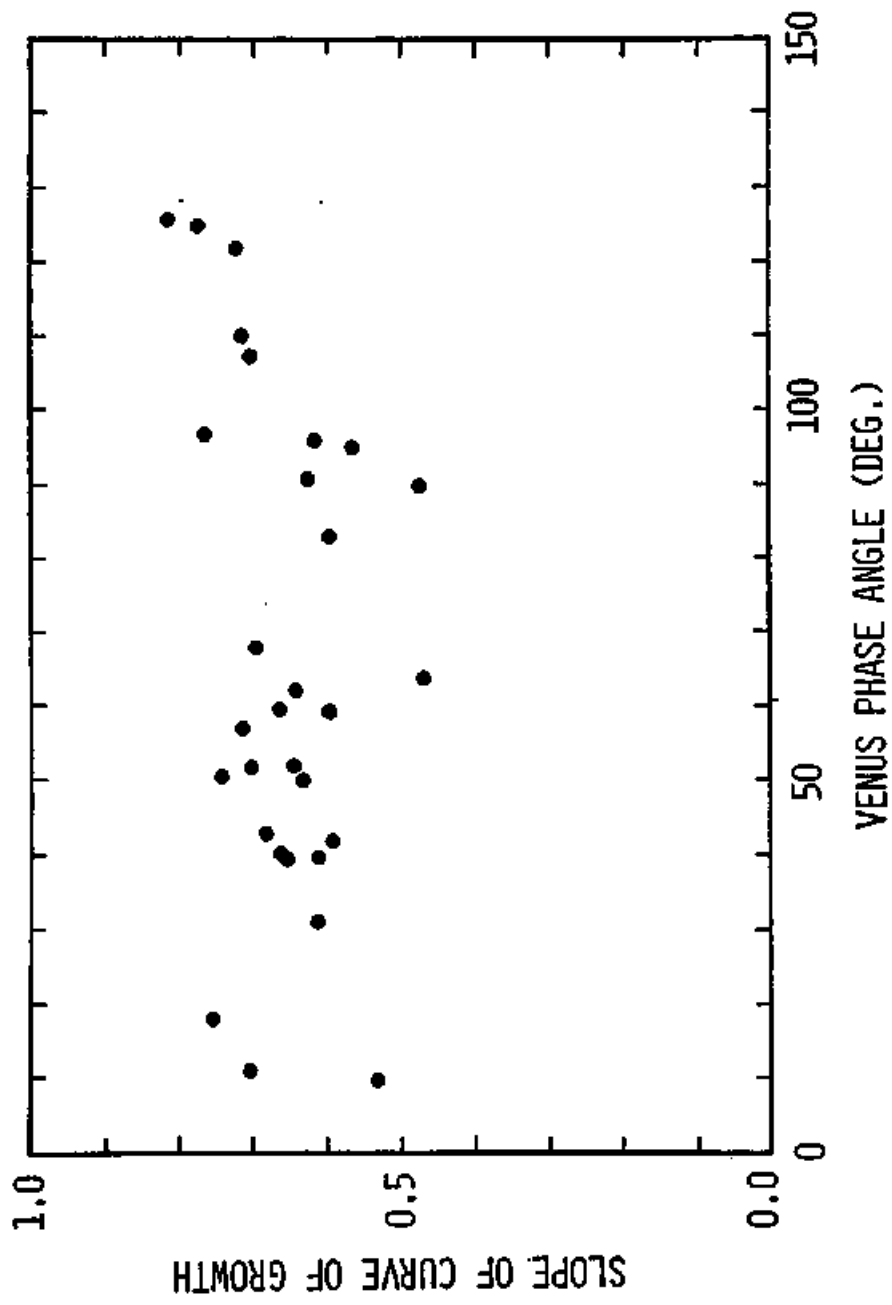


Fig. 5.